Full-field Strain Mapping of C-SiC Composites for Hypersonic Applications

S. Amini[1*] and F.W. Zok[2]
[1, 2] National Hypersonic Science Center, Materials Department
University of California, Santa Barbara, California, USA
[*]Currently at the United Technologies Research Center, East Hartford, Connecticut, USA

Keywords*: ceramic matrix composites, strain mapping, hypersonic flight, digital image correlation*

1. Introduction

Sustained hypersonic flights at high Mach numbers impose a range of high heat fluxes and heat loads that vary with position on the vehicle from those that can be sustained by current materials to those that cannot, even for brief times [1-2]. Ceramic matrix composites (CMCs) are the only class of materials so far identified as potentially capable of satisfying the system design requirements of high strength-to-weight ratio and operation with high surface temperatures [3-4]. Carbon fiber reinforced silicon carbide matrix composites (C-SiC) are the premier materials targeted for use in high-temperature applications of hypersonic flight vehicles, including wing leading edges and scramjet liners as well as in critical propulsion components such as turbine blisks, turbo-pump rotors, and nozzle exit ramps for advanced rocket engines [4-7]. The macroscopic behavior of CMCs depends not only on the properties of their individual constituents but also on the interaction between these phases, e.g. fiber and matrix, and also on their interface properties [8]. As material complexity evolves in CMCs to meet the extreme challenges of hypersonics, major shortcomings become critical in materials characterization, e.g. failure mechanisms, obscured by the difficulty of visualizing damage evolution during tests due to high temperatures. More importantly, the various fields of application and the complexity and heterogeneities in their microstructures – that can also obscure understanding the multiple interacting failure mechanisms – require better understanding of their micromechanical behavior under external loads. When complex CMCs such as C-SiC are subjected to external mechanical loads, the inhomogeneous strain localization due to waviness, may lead to the nucleation of failure of the fibers, of the matrix material, or to de-bonding effects at the interfaces between the matrix and the fibers preceding the actual global failure event [8-9]. The problem of predicting macroscopic elasticity and local strains remains a key issue for three-dimensional (3D) textile composites including C-SiC composites, particularly in load-critical applications. The difficulty is inherently related to the strong influence of the highly heterogeneous and locally anisotropic character of a textile composite on the distribution of stresses and strains. The physics of failure is also intimately associated with the discrete nature of the interlaced fiber tows in a textile composite. Many empirical and theoretical studies have been performed in order to identify the underlying micromechanical origin of such intricate and complex composite failure mechanisms and to propose solutions to improve the resistance against failure [8-11]. Better knowledge of the micromechanics of these materials under load will not only make these materials more useful but also contribute to an improvement in safety and design of the engineering components made from them for hypersonic applications.

In this work, tensile testing is coupled with the novel technique of surface strain mapping via digital image correlation (DIC) utilized for resolving the global mechanical behavior and spatial distribution of the strains in a 3-layer woven angle-interlock C-SiC composite. The DIC technique works by correlating the digital images of surface patterns before and after straining utilized as a powerful tool to map strain distributions at different length scales. This allows conducting a detailed investigation of complex micromechanical aspects that are associated with the distribution of the strain in a C-SiC heterogeneous material. DIC is a practical, effective and powerful tool for qualitative and quantitative deformation measurement in 3D, specifically for polymer matrix composites [12-17]. But there is little work done on woven ceramic matrix composites. The principal objectives of the present study are threefold: First, to implement a 3D

strain mapping system for probing the global mechanical response of a woven 3-layer angle interlock C-SiC composite; Second, to identify the degree of inhomogeneity of strains and ascertain whether periodic variations are consistent with the underlying tow architecture; Last, to identify differences in tensile behavior of such material subject to loading in the warp and weft directions and acquire strain distributions at different length scales ranging from length scales as small as the characteristic fiber tow dimensions up to the length scales as large as several unit cells of the weave structure.

2. Experimental Details

The composite samples are carbon fiber with SiC matrix, in which the reinforcement is a three-dimensional 3-layer angle-interlock weave. The composite was produced from a fiber preform consisting of carbon fiber tows (T300-6K) woven in a 3-layer angle-interlock architecture (Fig. 1). The preform was processed by chemical vapor infiltration to deposit a thin coating of pyrolytic carbon on the individual fibers and then to infiltrate SiC partially within the individual fiber tows to build up a layer of about 10 μm thick SiC encasing each tow. This layer was sufficient to form a continuous matrix that bonded all of the interwoven fiber tows together where they touched one another, while leaving distinct gaps between fiber tows in other regions. The tensile tests were performed at room temperature on tabbed rectangular specimens, 25 mm in width and 140 mm in length, prepared by laser-cutting. To determine full-field displacements, the specimens were covered with a random speckle pattern obtained by spraying white and black paints on the surface. The optical images were used in the digital image correlation model to determine the displacement fields and to obtain *in-situ* full-field strain maps during tension testing.

3. Results

3.1. Global Stiffness

The *Z*-profile of the specimens tested in the weft and warp directions superimposed on the speckled surfaces are shown in Fig. 2. Global strains were measured by DIC extensometry during tensile testing (Fig. 3a). The Initial elastic modulus is dictated by the fibers in the loading direction. Weft orientation response remains essentially linear up to fracture but warp orientation response exhibits significant non-linearity and greater strain to failure (0.95% vs. 0.6%). Also the elastic modulus (linear portion) in warp direction is considerably lower than that in the weft direction. These effects (differences in failure strain and stiffness knockdown) are attributed to the effects of warp tow waviness and straightening of the warp fiber tows during tensile loading. The amplitude of stiffness knockdown depends strongly on the degree of fiber waviness, being approximately proportional to the waviness [9]. More importantly, straightening of wavy tows in this material (without a fully dense matrix) can occur more readily than what might be expected for a woven fiber ceramic matrix composite with a stiff and fully dense ceramic matrix.

3.2. Local Stiffness and Gauge Averaging (Weft Direction)

Comparisons of strains measured along a single weft tow, averaged over a distance of either four entire unit cells (A-B) or over four individual unit cells (A-X, X-Y, Y-Z, Z-B [Fig. 2a]) shows that cell-to-cell local strain variations are about 15% (Fig. 3b). Note that each unit cell is comprised of four characteristic tow widths. On the other hand, weft strains are significantly greater than average by a factor of two in segments situated beneath surface warp tows (m-n, p-q, s-t and v-w [Fig. 2a]) as shown in Fig. 4a. However, weft strains in segments that are positioned beneath surface warp crowns with higher *Z*, e.g. v-w (Fig. 4b), exhibit smaller strains by ~ 40%. This knockdown is most likely attributable to the smaller degree of fiber waviness in segments such as v-w. More importantly, weft strains exhibit wide variability in those segments residing on the surface (n-o, o-X, X-p, etc. [Fig. 2a]) as shown in Fig. 5a. Note that negative strains are attributable to tow straightening during tensile testing. Large strain variability was also obtained in central row of weft tows (1-2, 3-4, 5-6, 7-8, 9-10, 11-12 [Fig. 2a]) as shown in Fig. 5b. These tows reside beneath the near surface weft tows. The strain knockdown in these weft tow segments as opposed to the surface weft tows (A-B) can be accounted for by the effects of tow waviness, being less in the former (e.g. 1-2, etc.).

3.3. Local Stiffness and Gauge Averaging (Warp Direction)

Strains in warp orientation (Fig. 2b) also show pronounced increasing variability as the length scale over which the strain is averaged is decreased. For instance, comparisons of strains measured along a single warp tow, averaged over a distance of one entire unit cell length (paths a-e in lines 1-4 [Fig. 2b]) shows that cell-to-cell local strain variations are close to naught as illustrated in Fig. 6a. Note that each unit cell length is comprised of eight characteristic tow widths. But when the length scale over which the strain is averaged is decreased to four characteristic tow widths (paths a-c and c-e in lines 1-4 [Fig. 2b]) and then subsequently to two characteristic tow widths (paths a-b, b-c, c-d and d-e in lines 1-4 [Fig. 2b]), then the strains exhibit significant increasing variability (Figs. 6b and 6c).

4. Discussion

Selecting length scales comparable with a characteristic fiber tow width allows assessing macroscopic mechanical performance of the structure and yet also allows prediction of variations in the local strains, which is essential to failure predictions at critical locations. Recent experimental and modeling observations in textile composites have also shown that most failure mechanisms are associated with a length scale that is comparable with a characteristic fiber tow dimension [8, 21]. Thus, the appropriateness of a tow-gauge as the length scale over which the local strain variations are measured here cannot be overemphasized. From an experimental point of view, large variations in the local strains could potentially be a major issue for the durability of thermal barrier coatings (TBCs) applied on the surface of C-SiC composites to prevent degradation. These large local strain variations could result in the initiation of cracks within the TBC system and consequently failure of the TBC system by delamination.

The macroscopic elastic properties measured here are significantly smaller than local strains measured at smaller length scales, mostly attributable to tow waviness. The macroscopic elastic properties determine structural performance prior to damage, but local stiffness and strains determine failure mechanisms, strength and life of structure. The results of this work can represent the physics of failure as opposed to homogenization methods [9, 22] that are only effective in evaluating the macroscopic elastic properties. Homogenization methods can give inaccurate assessments of the local strain variations because strains are averaged over distances larger than characteristic tow width dimensions thus rendering strength and failure predictions unreliable.

5. Concluding Remarks

Full-field 3D strain mapping enables unprecedented detail of strain distributions in woven fiber composites by digital image correlation. Experiments on a woven 3-layer angle-interlock C-SiC composite indicate that axial strains measured over a gauge length of a unit cell are reproducible from one cell to another in both weft and warp directions. However, strain measurements obtained over shorter gauge lengths exhibit significant variability, increasing with decreasing gauge length. Inhomogeneity of the woven structure and thus presence of various elastically dissimilar regions within the composite can play a significant role in those variations and on the singularities that arise in the elastic fields, the degree of which depends on the length scale.

Acknowledgment

This work is funded jointly by the United States Air Force Office of Scientific Research (AFOSR) and National Aeronautics and Space Administration (NASA). The experimental work was carried out at the AFOSR/NASA's National Hypersonic Science Center and Pratt & Whitney's Center of Excellence in Composites at the University of California, Santa Barbara.

References

1. Rivers, H.K. and D.E. Glass. *Advances in hot-structure development*. in *5th European Workshop Thermal Protection Systems and Hot Structures, May 17, 2006 - May 19, 2006*. 2006. Noordwijk, Netherlands: European Space Agency.
2. Glass, D.E. *Ceramic Matrix Composite (CMC) Thermal Protection Systems (TPS) and Hot Structures for Hypersonic Vehicles*. in *15th AIAA Space Planes and Hypersonic Systems and Technologies Conference*.
3. Valdevit, L., et al., *A materials selection protocol for lightweight actively cooled panels.* Journal of Applied Mechanics, Transactions ASME, 2008. 75(Compendex): p. 0610221-06102215.

4. Van Wie, D.M., et al. *The hypersonic environment: Required operating conditions and design challenges*. 2004: Kluwer Academic Publishers.
5. Verrilli, M.J., et al., *Effect of environment on the stress-rupture behavior of a carbon-fiber-reinforced silicon carbide ceramic matrix composite.* Journal of the American Ceramic Society, 2004. 87(Compendex): p. 1536-1542.
6. Schmidt, S., et al., *Ceramic matrix composites: A challenge in space-propulsion technology applications.* International Journal of Applied Ceramic Technology, 2005. 2(Compendex): p. 85-96.
7. Schmidt, S., et al. *Advanced ceramic matrix composite materials for current and future propulsion technology applications*. 2004: Elsevier Ltd.
8. Yang, Q.D., et al., *Evaluation of macroscopic and local strains in a three-dimensional woven C/SiC composite.* Journal of the American Ceramic Society, 2005. 88(Compendex): p. 719-725.
9. Cox, B.N. and M.S. Dadkhah, *Macroscopic elasticity of 3D woven composites.* Journal of Composite Materials, 1995. 29(Compendex): p. 785-819.
10. Cox, B.N., M.S. Dadkhah, and W.L. Morris, *On the tensile failure of 3D woven composites.* Composites Part A: Applied Science and Manufacturing, 1996. 27(6): p. 447-458.
11. Cox, B.N., et al., *Failure mechanisms of 3D woven composites in tension, compression, and bending.* Acta Metallurgica Et Materialia, 1994. 42(12): p. 3967-3984.
12. Battley, M. and M. Burman, *Characterization of ductile core materials.* Journal of Sandwich Structures and Materials, 2010. 12(Compendex): p. 237-252.
13. Ivanov, D.S., et al., *A comparative study of tensile properties of non-crimp 3D orthogonal weave and multi-layer plain weave E-glass composites. Part 2: Comprehensive experimental results.* Composites Part A: Applied Science and Manufacturing, 2009. 40(Compendex): p. 1144-1157.
14. De Almeida, O., F. Lagattu, and J. Brillaud, *Analysis by a 3D DIC technique of volumetric deformation gradients: Application to polypropylene/EPR/talc composites.* Composites Part A: Applied Science and Manufacturing, 2008. 39(Compendex): p. 1210-1217.
15. Lomov, S.V., et al., *A comparative study of tensile properties of non-crimp 3D orthogonal weave and multi-layer plain weave E-glass composites. Part 1: Materials, methods and principal results.* Composites Part A: Applied Science and Manufacturing, 2009. 40(Compendex): p. 1134-1143.
16. Littell, J.D., et al., *Characterization of damage in triaxial braided composites under tensile loading.* Journal of Aerospace Engineering, 2009. 22(Compendex): p. 270-279.
17. Lomov, S.V., et al., *Full-field strain measurements for validation of meso-FE analysis of textile composites.* Composites Part A: Applied Science and Manufacturing, 2008. 39(Compendex): p. 1218-1231.
18. Cox, B.N., W.C. Carter, and N.A. Fleck, *A binary model of textile composites--I. Formulation.* Acta Metallurgica Et Materialia, 1994. 42(10): p. 3463-3479.
19. Cox, B.N., W.C. Carter, and N.A. Fleck, *Binary model of textile composites - I. Formulation.* Acta Metallurgica Et Materialia, 1994. 42(Compendex): p. 3463-3479.
20. Xu, J., et al., *Binary model of textile composites - II. The elastic regime.* Acta Metallurgica Et Materialia, 1995. 43(Compendex): p. 3511-3524.
21. Yang, Q. and B. Cox, *Spatially averaged local strains in textile composites via the binary model formulation.* Journal of Engineering Materials and Technology, Transactions of the ASME, 2003. 125(Compendex): p. 418-425.
22. Naik, N.K. and B.J. Thuruthimattam, *Behavior of 3-D Orthogonally Woven Composites under Tensile Loading.* Journal of Composites Technology and Research, 1999. 21(Compendex): p. 153-163.

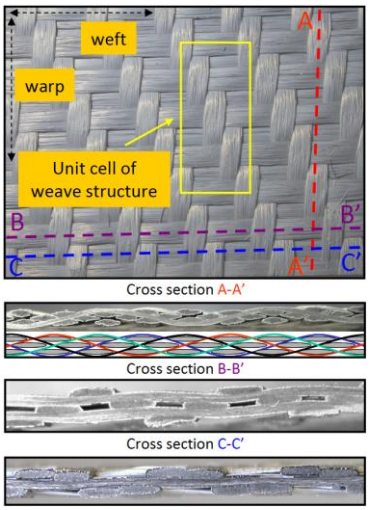

Fig. 1: Optical micrographs of the surface and various cross sections of the C-SiC 3-layer angle-interlock architecture.

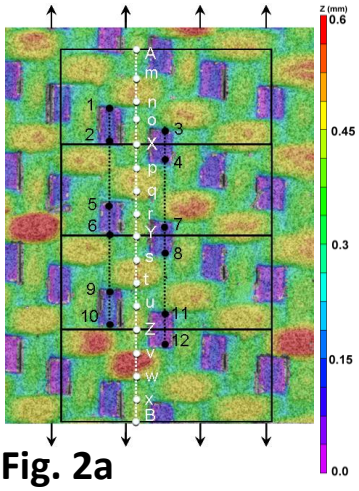

Fig. 2a

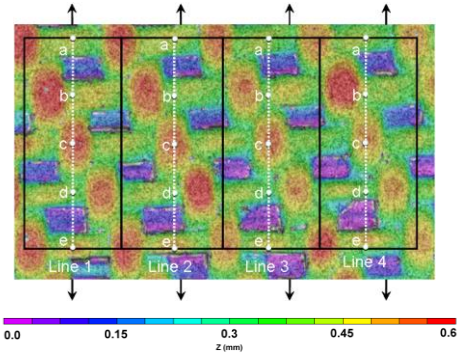

Fig. 2b

Fig. 2: The *Z*-profile of the specimen tested in the, a) weft, and, b) warp, directions.

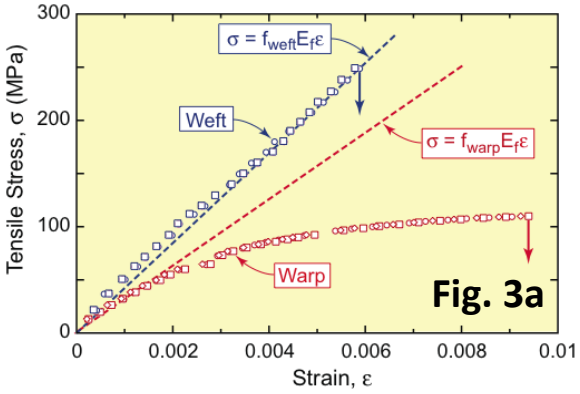

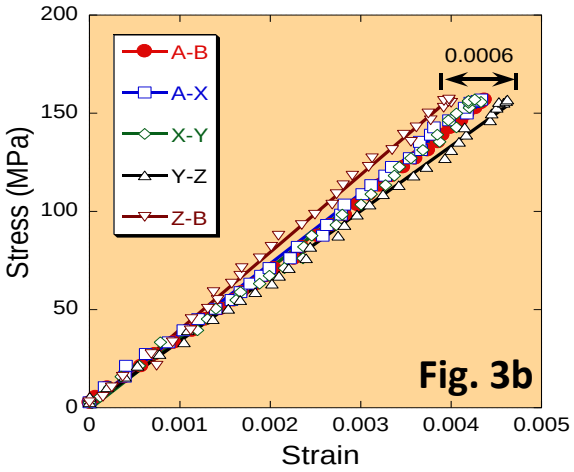

Fig. 3: a) Global strains measured by DIC extensometry during tensile testing; b) Comparisons of strains measured along a single weft tow, averaged over a distance of either four entire unit cells or four individual unit cells.

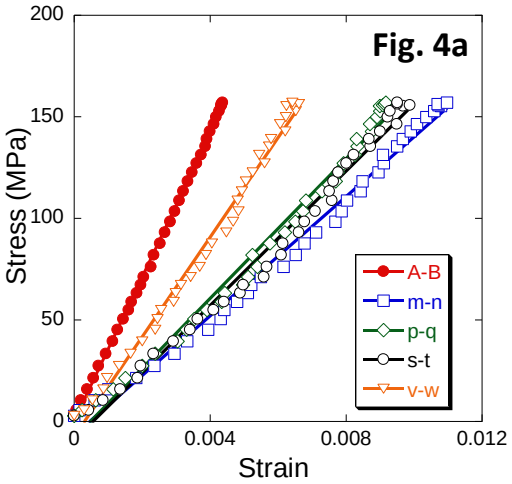

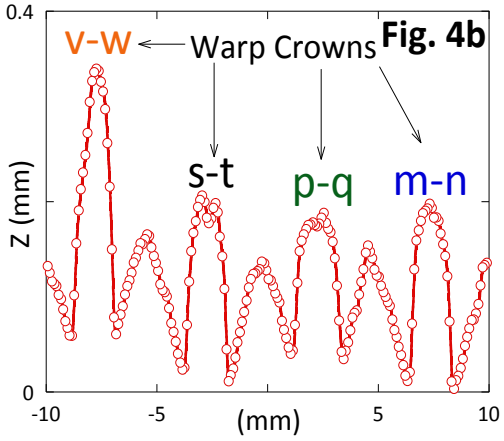

Fig. 4: a) Weft strains in segments situated beneath surface warp tows; b) The Z-profile of a single weft tow (A-B) illustrating the position and height of the surface warp crowns.

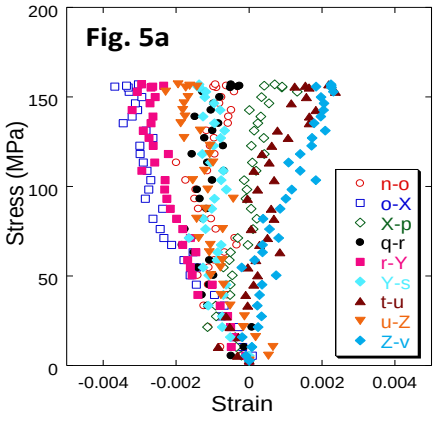

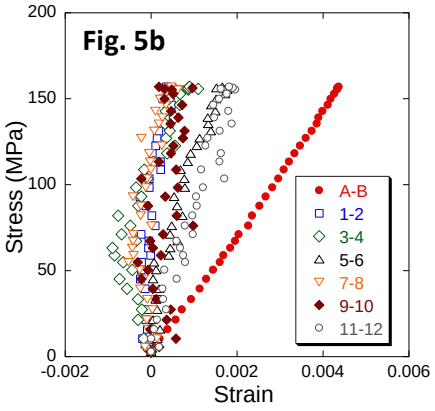

Fig. 5: Variability of strains in, a) weft segments residing on the surface, and, b) those in the central row of weft tows.

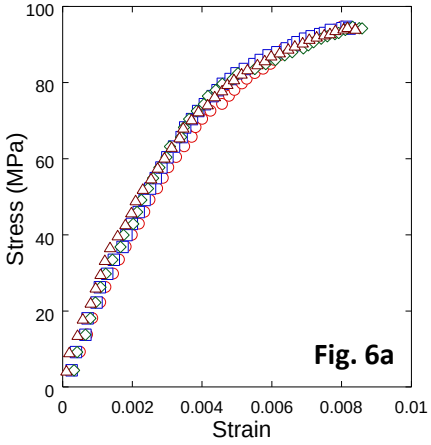

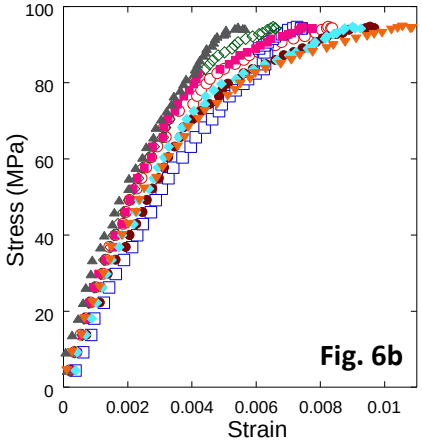

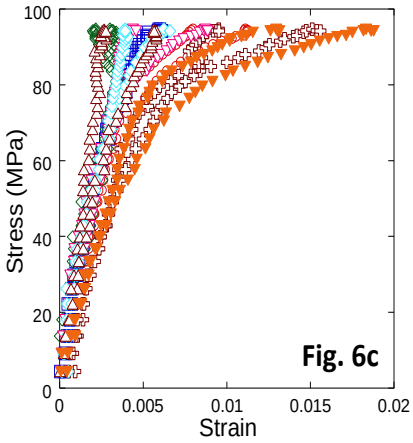

Fig. 6: Strains measured along a single warp tow, averaged over a distance of, a) one entire unit cell, b) four characteristic tow widths, and, c) two characteristic tow widths exhibiting significant increasing variability.